International Journal of Engineering and Advanced Technology (IJEAT)
ISSN: 2249-8958 (Online), Volume-3 Issue-1, October 2013

A Fault Location Technique for Transmission Lines Using Phasor Measurements

Abdolhamid Rahideh, Mohsen Gitizadeh, Sirus Mohammadi

Abstract*— This paper presents a fault location technique for two-terminal multisection compound transmission lines, which combine overhead lines with underground power cables, using synchronized phasor measurements acquired by global positioning system (GPS) based phasor measurement units (PMUs) or digital relays with embedded PMU or by fault-on relay data synchronization algorithms. The technique is extended from a two-terminal fault location method with synchronized phasormeasurements as inputs. A novel fault section selector is proposedto select the fault line section in advance. The proposed techniquehas the ability to locate a fault no matter where the fault is on overhead line or underground power cable. The adopted technique has a solid theoretical foundation and is direct and simple in terms of computational complexity. Both extensive simulation results and field test results are presented to demonstrate the effectiveness of the proposed scheme. The proposed technique has already been implemented in the Taiwan power system since the year 2008. Up to the present, the proposed technique yields excellent performance in practice.

***Index Terms*—Fault location, phasor measurement units (PMUs), two-terminal compound transmission lines.**

I. INTRODUCTION

In electrical utilities, transmission lines form the backbone of power systems. With regard to reliability and maintenance costs of power delivery, accurate fault location for transmission lines is of vital importance in restoring power service, and reducing outage time as much as possible. Many fault location techniques have been proposed in open literature [1]–[22]. Among these techniques, specifically Takagi et al. [5], [6] applied the superposition principle to estimate single-ended fault location algorithms. The said authors' approaches were very attractive as they did not require communication to obtain results. However, algorithms based on singleended data will affect accuracy due to variations in source impedances, fault incidence angle, fault impedance, and loading conditions.With the advent of global positioning system (GPS)-based synchronously measuring units including phasor measurement units (PMUs) [23], digital relays, and digital fault recorders in the early 1990s, GPS-based fault location techniques[2], [7]–[17] have become promising. The main advantage of GPS-based techniques is that fault location estimation accuracy is unaffected by variations in source impedances and fault impedances due to the availability of two-terminal synchronized data. Kezunovc *et al.* [7], [8] employed synchronized voltages and currents samples at two terminals to estimate the fault location. They adopted a time-domain model as basis for the algorithm development. However, data must be acquired at a sufficiently high sampling rate to provide adequate approximation of the derivatives. For their part, Lee *et al.* [9] utilized synchronized phasors at both terminals to obtain the fault location. Their algorithm was based on positive and zero sequence components of postfault voltages and currents. In particular, errors will be presented when dealing with three-phase faults where zero sequence components are absent. Moreover, their work only considered a short line model that could not reflect the nature of transmission lines. Meanwhile, our previous works [10]–[14] proposed fault location/detection techniques for transmission lines using synchronized phasor measurements. The developed fault location/detection indices can be used for transmission line protection as well [15]–[17]. However, due to the high installation cost of PMUs, majority of utilities install PMUs only at key substations. Thus, the digital measurements at two line terminals are acquired asynchronously in the absence of GPS signal. Therefore, fault location estimation based on two-terminal data will suffer in terms of accuracy. Consequently, fault locations based on post fault data synchronization algorithms were considered in some papers. Girgis *et al.* [18] used an iterative method to achieve time synchronization. The fault location method proposed by Dalcastagnê *et al.* [19] was based on voltage magnitudes. The proposed work [20] used the imaginary part of the fault locationindex to synchronize the measurements. To achieve a compromise between construction cost and environmental protection in Taiwan, overhead lines combined with underground cables have been widely adopted by the Taiwan Power Company (Taipower) with 161 kV and 345 kV transmission systems. However, the developed techniques [1]–[20] cannot locate the fault accurately using these kinds of compound lines. Thus, a two-terminal multisection line model must be considered to develop a new fault location method. Gilany *et al.* [21] used synchronized measurements to detect/locate a fault for a two-section line combined an overhead line with an underground power cable section. Their work required identifying the fault type before locating a fault. Meanwhile, their method is applicable only to two-section compound transmission lines instead of more general multisection compound lines.

Manuscript published on 30 October 2013.
***** Correspondence Author (s)
Abdolhamid Rahideh, Department of Electrical Egineering, College of Graduate Studies, Science and Research Branch Kohgiluyeh and Boyer-ahmad, Islamic Azad University, Yasouj, Iran.
Mohsen Gitizadeh, Department of Electrical and Electronic Engineering, Shiraz University of Technology, Shiraz, Iran.
Sirus Mohammadi, Deparment of Electrical Engineering, Islamic Azad University Gachsaran, Branch Gachsaran, Iran.

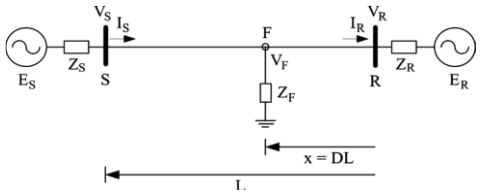

Fig. 1. Single line diagram of a single-circuit transposed transmission line with a fault at a distance x=DL away from the bus R

Yang *et al.* [22] adopted distributed parameter line models and the Newton-Raphson iteration to locate a fault for multisection underground cables. Since the Newton-Raphson iterative operation is required, the scheme suffers from convergence issues. Moreover, their method did not consider more generally combined overhead lines with power cables, such as the case considered in the current study. This paper proposes an innovative fault location technique for two-terminal multisection compound transmission lines. The

proposed scheme provides a novel selector to distinguish the internal fault of a compounded line from an external fault as well as to identify the accurate fault line section of an internal

fault. The proposed scheme can thus yield an exact solution for fault location estimation of a multi section line to avoid the complexity of multi solution computations.

II. FAULT LOCATION TECHNIQUE

A. Review of Two-Terminal Fault Location Technique

Fig. 1 shows a single-circuit transposed transmission line. In Fig. 1, total line length between buses S and R is assumed to be L, and the synchronized voltage and current phasors measured and the synchronized voltage and current phasors measured S and R are V_s, I_s, V_R and I_R, respectively.

Using symmetrical components transformation to decouple three-phase quantities [25] and to consider only the variation of a distance variable x (km), the relation between the voltages and currents at a distance x away from bus R can be expressed by the following sequence equations [25]:

$$\frac{dV_{012}}{dx} = Z_{012} I_{012} \qquad (1)$$

$$\frac{dI_{012}}{dx} = Y_{012} V_{012} \qquad (2)$$

Where Z_{012} and Y_{012} are the per-unit length sequence impedance (Ohm/km) and admittance (Mho/km) of the transmission line, respectively. The matrices of Z_{012} and Y_{012} are all diagonal matrices, and the diagonal entries of matrices Z_{012} and Y_{012} are (Z_0,Z_1,Z_2) and (Y_0,Y_1,Y_2), respectively. Furthermore, $I_{012} = [I_0 \ I_1 \ I_2]^T$ and $V_{012} = [V_0 \ V_1 \ V_2]^T$. The variables with the subscripts 0, 1, 2 denote the zero-, positive-, and negative-sequence variables, respectively.

The solutions of voltages and currents of the three decoupled sequence systems can be written as [10], [11]

$$V_{xi} = A_i \exp(\Gamma_i x) + B_i \exp(-\Gamma_i x) \qquad (3)$$

$$I_{xi} = \frac{1}{Z_{ci}} [A_i \exp(\Gamma_i x) - B_i \exp(-\Gamma_i x)] \qquad (4)$$

where the subscript i denotes 0, 1, and 2 sequence variables, $Z_{ci} = \sqrt{Z_i / Y_i}$ denotes the characteristic impedance, and $\Gamma_i = \sqrt{Z_i Y_i}$ is the propagation constant. The constants A_i and B_i can be obtained by the boundary conditions of voltages and currents measured at bus R and bus S , respectively. Therefore, voltage (3) can be further rewritten as

$$V_{xi,R} = \frac{(V_{i,R} + Z_{Ci} I_{i,R})}{2} e^{\Gamma_i x} + \frac{(V_{i,R} - Z_{Ci} I_{i,R})}{2} e^{-\Gamma_i x} \qquad (5)$$

$$V_{xi,S} = \frac{1}{2} e^{-\Gamma_i L} (V_{i,S} + Z_{Ci} I_{i,S}) e^{\Gamma_i x} + \frac{1}{2} e^{\Gamma_i L} (V_{i,S} - Z_{Ci} I_{i,S}) e^{-\Gamma_i x}. \qquad (6)$$

Equations (5) and (6) represent the voltages at point x, which are expressed in terms of the two data sets ($V_{i,R}$, $I_{i,R}$) and ($V_{i,s}$, $I_{i,s}$) measured at the receiving end R and sending end S of the line, respectively. Meanwhile, the positive-sequence quantities can respond to all fault types; thus, they are chosen to determine the fault locations in the current study to avoid fault type identification. For ease of illustration, subscript i=l, which denotes the positive-sequence quantities, is dropped. A fault is assumed to occur at point F with a distance x=DL km away from the receiving end R on a transmission line shown in Fig. 1, where D is termed as the per-unit fault location index. Using the relationship $V_{F,R} = V_{F,S}$ and equating (5) to (6), the index can be solved as follows [10]–[12]:

$$D = \frac{\ln\left(\frac{N}{M}\right)}{2\Gamma L} \qquad (7)$$

Where M and N are given by

$$M = \frac{1}{2}(V_S + Z_C I_S) e^{-\Gamma L} - \frac{1}{2}(V_R + Z_C I_R) \qquad (8)$$

$$N = \frac{1}{2}(V_R - Z_C I_R) - \frac{1}{2}(V_S - Z_C I_S) e^{\Gamma L}. \qquad (9)$$

When a fault occurs between buses S and R, the obtained Value D of is between 0 and 1. When no fault or an external fault occurs, the value of D is indefinite. It is worth mentioning that there is no assumption made in the procedure of derivation for the fault location index D. Thus, D the index is unaffected by the variations in source impedance, loading change, fault impedance, fault inception angle, and fault type.

B.Fault Location Technique for Two-Terminal Multi-Section Compound Transmission Lines

1) *Two-Section Compound Lines*: First, we consider a two section compound transmission line in which a section of overhead line is connected with the other section of underground power cable, as shown in Fig. 2. PMUs or digital relays are assumed to be installed at buses S and R. Therefore, we can acquire two-terminal synchronized voltage and current phasors using GPS technique or fault-on relay data synchronization algorithms.

Published By:
Blue Eyes Intelligence Engineering
and Sciences Publication (BEIESP)

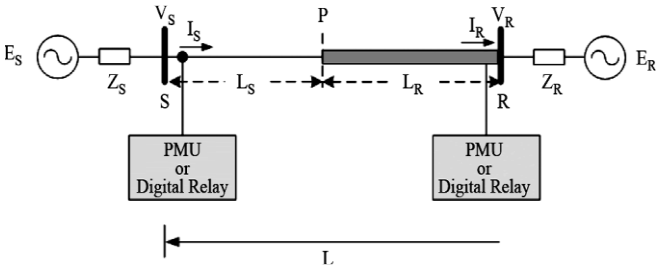

Fig. 2. One line diagram of a two-section compound transmission line; the thin line denotes the overhead line and the bold line denotes the power cable.

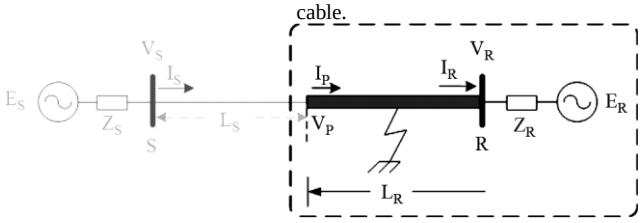

Fig. 3. A fault on the underground power cable section.

Lengths of the overhead line and underground power cable are denoted as L_S and L_R , respectively. Total line length between buses S and R is L . Tap point P of the transmission line is selected as the junction point between the L_S and L_R ,which can be defined as the virtual receiving end of the overhead line or the virtual sending end of the cable. A nonuniform line impedance is obtained in this case due to the nature of compound lines. For example, the surge impedance of the cable is approximately 10% of that of an overhead line [26]. The proposed fault location technique in this case is expressed using the following steps:

Step 1: ***Assume a fault on the right side of tap point P.*** As shown in Fig. 3, we assume that the fault is situated on the underground power cable L_R . Since the healthy section is the overhead line L_S , the voltage and current at any point in the overhead line can be derived by applying boundary conditions of bus S into (3) and (4). Consequently, we can obtain the voltage and current phasors at tap point P in terms of the sending end data sets (V_S,I_S) as

$$V_{P,S} = \frac{1}{2}e^{-\Gamma_S L_S}(V_S + Z_{C,S}I_S) + \frac{1}{2}e^{\Gamma_S L_S}(V_S - Z_{C,S}I_S) \quad (10)$$

$$I_{P,S} = \frac{1}{Z_{C,S}}\left[\frac{1}{2}e^{-\Gamma_S L_S}(V_S + Z_{C,S}I_S) - \frac{1}{2}e^{\Gamma_S L_S}(V_S - Z_{C,S}I_S)\right] \quad (11)$$

Where $Z_{C,S} = \sqrt{Z_S/Y_S}$ and $\Gamma_S = \sqrt{Z_S Y_S}$ denote the characteristic impedance and the propagation constants of the overhead line section, respectively. Z_S and Y_S are the positive sequence impedance and admittance of the L_S , respectively.

Now we derive the fault location index, using voltage and current phasors at tap point and bus and the line length . Substituting , expressed in (10), (11) into , in (6) and equating (5) to the newly derived (6) with the characteristic impedance, $Z_{C,R}$ and the propagation constant, Γ_R for the power cable section, respectively, the fault location index D_1 can be obtained as follows:

$$D_1 = \frac{\ln\left(\frac{N_R}{M_R}\right)}{2\Gamma_R L_R} \quad (12)$$

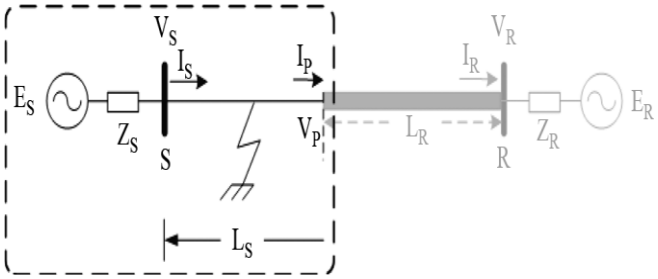

Fig. 4. A fault on the overhead line section.

where, $\Gamma_R = \sqrt{Z_R Y_R}$ in which Z_R and Y_R are respectively the positive sequence impedance and admittance of the underground power cable L_R.M_R and N_R are given by

$$M_R = \frac{1}{2}(V_{P,S} + Z_{C,R}I_{P,S})e^{-\Gamma_R L_R} - \frac{1}{2}(V_R + Z_{C,R}I_R) \quad (13)$$

$$N_R = \frac{1}{2}(V_R - Z_{C,R}I_R) - \frac{1}{2}(V_{P,S} - Z_{C,R}I_{P,S})e^{\Gamma_R L_R} \quad (14)$$

Where $Z_{C,R} = \sqrt{Z_R/Y_R}$.

Step 2: ***Assume a fault on the left side of tap point P.*** We assume that the fault occurs on the overhead line L_S , as shown in Fig. 4. Given the healthy section of the cable L_R, we can similarly derive the voltage and current phasors at P in terms of the receiving end data (V_R, I_R)

$$V_{P,R} = \frac{(V_R + Z_{C,R}I_R)}{2}e^{\Gamma_R L_R} + \frac{(V_R - Z_{C,R}I_R)}{2}e^{-\Gamma_R L_R} \quad (15)$$

$$I_{P,R} = \frac{1}{Z_{C,R}}\left[\frac{(V_R + Z_{C,R}I_R)}{2}e^{\Gamma_R L_R} - \frac{(V_R - Z_{C,R}I_R)}{2}e^{-\Gamma_R L_R}\right]. \quad (16)$$

Now we derive the fault location index, D_2 using voltage and current phasors at tap point P and bus S and the line length L_S . Substituting $V_{P,R}$,$I_{P,R}$ expressed in (15), (16) into , in (5) and equating (6) to the newly derived (5) with the characteristic impedance, $Z_{C,S}$ and the propagation constant, Γ_S for the overhead line section, respectively, the fault location index D_2 can be obtained as follows:

$$D_2 = \frac{\ln\left(\frac{N_S}{M_S}\right)}{2\Gamma_S L_S} \quad (17)$$

Where

$$M_S = \frac{1}{2}(V_S + Z_{C,S}I_S)e^{-\Gamma_S L_S} - \frac{1}{2}(V_{P,R} + Z_{C,S}I_{P,R}) \quad (18)$$

Published By:
Blue Eyes Intelligence Engineering
and Sciences Publication (BEIESP)

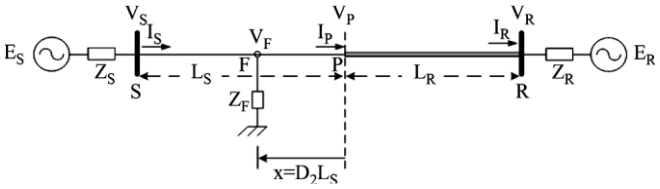

Fig. 5. A fault occurs at a distance $x=D_2L_S$ away from tap point P .

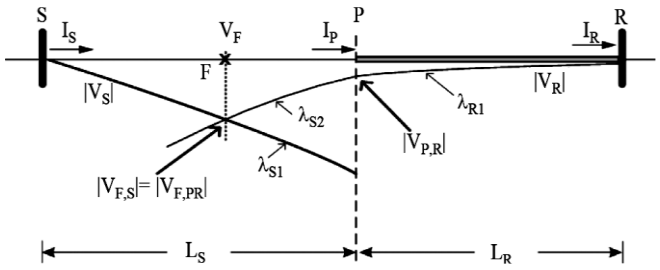

Fig. 6. Relationship between the curves of $|V_S|$ and $|VR|$ when calculating D_2.

$$N_S = \frac{1}{2}(V_{P,R} - Z_{C,S}I_{P,R}) - \frac{1}{2}(V_S - Z_{C,S}I_S)e^{\Gamma_S L_S}. \quad (19)$$

Step 3: ***Faulted section identification/fault location estimation.*** Suppose that a fault occurs at the point with a distance of $x=D_2L_S$ km away from tap point P on the L_S section of a transmission line shown in Fig. 5.

We know that the voltage magnitudes and angles at the fault point F obtained from the quantities of two terminals are equal when using synchronized measurements. For ease of illustration, we only draw the two voltage magnitude profiles derived from buses S and R, as shown in Fig. 6. In Fig. 6, λ_{S1} denotes the curve for the variation of $|V_S|$;λ_{R1} and λ_{R2} denote the two parts of the curve for the variation of $|V_R|$ on the L_R and L_S sections, respectively. Note that the slopes of λ_{R1} and λ_{R2} are different because the line impedances of the L_R and the L_S sections are not uniform. Moreover, the curves of $|V_S|$ and $|V_R|$ are both almost linearly decreased from buses and orienting to the fault position [28].

As shown in Fig. 6, the intersection point of the curves λ_{S1} and λ_{R2} pertains to the amplitude of the fault voltage V_F . By using the relationship $|V_{F,PR}|=|V_{F,S}|$ or $V_{F,PR}=V_{F,S}$ as mentioned in *Step 2*, the index D_2 can be obtained as shown in (17), where $V_{F,PR}$ and $V_{F,S}$ are derived from rewriting (5) and (6) as

$$V_{F,PR} = \frac{(V_{P,R} + Z_{C,S}I_{P,R})}{2}e^{\Gamma_S D_2 L_S} + \frac{(V_{P,R} - Z_{C,S}I_{P,R})}{2}e^{-\Gamma_S D_2 L_S} \quad (20)$$

$$V_{F,S} = \frac{1}{2}e^{-\Gamma_S L_S}(V_S + Z_{C,S}I_S)e^{\Gamma_S D_2 L_S} + \frac{1}{2}e^{\Gamma_S L_S}(V_S - Z_{C,S}I_S)e^{-\Gamma_S D_2 L_S} \quad (21)$$

Where $V_{P,R}$ and $I_{P,R}$ are expressed in (15) and (16), respectively. Since the index D_2 , which is termed as the per-unit fault location index, is in reference with tap point P and the L_s is defined as reference per-unit length, the obtained value D_2 is obviously in the interval [0,1].

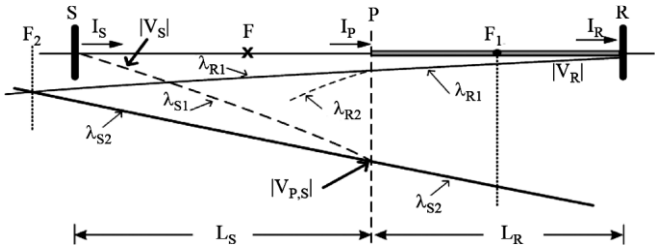

Fig. 7. Relationship between the curves of$|V_S|$ and $|V_R|$ when calculating D_1.

TABLE I
THE FAULTED SECTION/FAULT LOCATION IDENTIFICATION FOR TWO-SECTION COMPOUND TRANSMISSION LINES

(1) $D_2 < 0$ and $0 \leqq D_1 < 1$: the fault occurs on L_R and D_1 is the actual fault location away from bus R.
(2) $0 < D_2 \leqq 1$ and $D_1 > 1$: the fault occurs on L_S and $(1-D_2)$ is the actual fault location away from bus S.
(3) $D_2 = 0$ and $D_1 = 1$: the fault occurs at the point P.

Meanwhile, the index D_1 shown in (12) is obtained by assuming a fault on the right side (the cable section) of tap point P . The relationship between the curves of and for this case is illustrated in Fig. 7.

Since the curves of $|V_s|$ and $|V_R|$ are both decreased from buses S and R orienting to the correct fault position [28], in a similar manner, one can clearly observe that the curves λ_{R1} and λ_{S2} (with λ_{S2} being part of the curve$|V_S|$ in the L_R section) shown in Fig. 7 will not have any intersection points on the L_R section. Instead, as the fault is assumed on the L_R section, the slopes of curves λ_{R1} and λ_{S2} are thus extended to the L_S section to calculate the index D_1 as shown in Fig. 7. As a result, the curve λ_{R1} will intersect with curve λ_{S2} at the point F_2. This fact indicates that the index D_1 certainly converges on a value larger than 1 because the index D_1 is with respect to bus R (as a reference) and the line length L_R is defined as reference per-unit length. However, the derived fault point F_2 is incorrect because the correct curves of $|V_R|$ and $|V_S|$ on the L_S section are λ_{R2} and λ_{S1}, respectively. Based on the foregoing discussions, we conclude that if the index D_2 is in the interval[0,1] and the index D_1 is larger than 1, one can identify that the fault occurs on the section of a two-section compound line, such as in Fig. 5. In a similar manner, we can determine the relationships between the two indices,D_1 and D_2 , when dealing with a fault on the L_R section or at tap point P . All the specific relationships between the two indices D_1 and D_2 from which one can identify the faulted line section/fault location are Summarized in Table I. Based on a similar process, we will develop a technique for the identification of the faulted section/fault location with general multi section compound lines in the next subsection.

1) *Two-Terminal N-Section(N>=2) Compound Lines:*In practice, the structure of compound transmission line systems is usually more complicated than the two-section case mentioned above. Now we move to more general multisection compound transmission line cases. Consider an N-section (N>=2)compound line depicted in Fig. 8. PMUs or digital relays are installed at sending bus and receiving bus .

Published By:
Blue Eyes Intelligence Engineering
and Sciences Publication (BEIESP)

Therefore, we can obtain the synchronized voltage and current phasors at both terminals of the considered system. The length of every sectionis denoted as L_1, L_2,…, L_{N-1} and L_N. *Every line* section may be composed by either an overhead line or an underground power cable. Two consecutive line sections may be either overhead lines, both underground cables, or an overhead line with an underground cable. For example, L_1 and L_2 in Fig. 8 are both overhead lines, but their line impedances are very different (the conductor L_1 of may be ACSR795D, while the conductor of may be ACSR636D)

The proposed fault location scheme for general two-terminal N-section compound transmission lines can be composed of two portions:

The N Fault Location Indices Derivation: In order to illustrate the proposed fault location technique in a convenient manner, suppose first that a fault occurs at the point F, which is x km away from the receiving end R and L on the section of a transmission line shown in Fig. 8. The line length L_1 is defined as reference length of the derived fault location indices. The fault location scheme for the fault on the L_3 section is divided into three procedures, as described below:

Procedure 1: Derive voltage/current phasors at point $P_{3,R}$

As shown in Fig. 8, since the sections L_1 and L_2 are both healthy, the voltage and current at any point on the L_1 or L_2 can be derived by applying boundary conditions of bus R into (3) and (4) in terms of the line parameters of the L_1 or L_2 . As a result, the voltage and current phasors($V_{P3,R}$, $I_{P3,R}$) at tap point $P_{3,R}$ can be derived using successive algebraic substitution steps from the data sets(V_R, I_R) at receiving end R. This is expressed in matrix form as follows:

$$\begin{bmatrix} V_{P3,R} \\ I_{P3,R} \end{bmatrix} = T_{R2} \cdot T_{R1} \cdot \begin{bmatrix} V_R \\ I_R \end{bmatrix} \qquad (22)$$

where T_{R1} and T_{R2} are defined as the phasor transformation matrices of bus R and the subscripts 1 and 2 denote the use of the line parameters of the L_1 and L_2 sections, respectively. The general form of the matrix T_R is given as the following:

$$T_{Rm} = \frac{1}{2}\begin{bmatrix} e^{\Gamma_{Lm}L_m}+e^{-\Gamma_{Lm}L_m} & Z_{C,Lm}\cdot(e^{\Gamma_{Lm}L_m}-e^{-\Gamma_{Lm}L_m}) \\ \frac{e^{\Gamma_{Lm}L_m}-e^{-\Gamma_{Lm}L_m}}{Z_{C,Lm}} & e^{\Gamma_{Lm}L_m}+e^{-\Gamma_{Lm}L_m} \end{bmatrix} = \begin{bmatrix} \cosh(\Gamma_{Lm}L_m) & Z_{C,Lm}\cdot\sinh(\Gamma_{Lm}L_m) \\ \frac{\sinh(\Gamma_{Lm}L_m)}{Z_{C,Lm}} & \cosh(\Gamma_{Lm}L_m) \end{bmatrix} \qquad (23)$$

Where $Z_{C,Lm}$ and Γ_{Lm} are the positive sequence characteristic impedance and propagation constant for the L_m section, respectively.

Procedure 2: Derive voltage/current phasors at point

Since the L_N, L_{N-1},…,L_5 and L_4 are all healthy sections, we can likewise derive the voltage and current phasors ($V_{P3,S}$, $I_{P3,S}$) at tap point $P_{3,S}$ in Fig. 8 via a series of substitutions from the data sets at sending end S using the following relations:

$$\begin{bmatrix} V_{P3,S} \\ I_{P3,S} \end{bmatrix} = T_{S4} \cdot T_{S5} \cdot \cdots \cdot T_{S(N-1)} \cdot T_{SN} \cdot \begin{bmatrix} V_S \\ I_S \end{bmatrix} \qquad (24)$$

where T_{S4},T_{S5},…,$T_{S(N-1)}$ and T_{SN} are defined as the phasor transformation matrices of bus S . The general form of the matrix T_S is shown below:

$$T_{Sm} = \frac{1}{2}\begin{bmatrix} e^{\Gamma_{Lm}L_m}+e^{-\Gamma_{Lm}L_m} & -Z_{C,Lm}\cdot(e^{\Gamma_{Lm}L_m}-e^{-\Gamma_{Lm}L_m}) \\ \frac{-(e^{\Gamma_{Lm}L_m}-e^{-\Gamma_{Lm}L_m})}{Z_{C,Lm}} & e^{\Gamma_{Lm}L_m}+e^{-\Gamma_{Lm}L_m} \end{bmatrix} = \begin{bmatrix} \cosh(\Gamma_{Lm}L_m) & -Z_{C,Lm}\cdot\sinh(\Gamma_{Lm}L_m) \\ \frac{-\sinh(\Gamma_{Lm}L_m)}{Z_{C,Lm}} & \cosh(\Gamma_{Lm}L_m) \end{bmatrix}. \qquad (25)$$

Procedure 3: fault location indices computation The application of the two-terminal fault location technique to solve for fault location x'=D_3L_3 away from the receiving end $P_{3,R}$ using two-terminal data sets ($V_{P3,R}$, $I_{P3,R}$) and ($V_{P3,S}$, $I_{P3,S}$) expressed in (22) and (24) is shown as follows:

$$D_3 = \frac{\ln\left(\frac{N_3}{M_3}\right)}{2\Gamma_{L3}L_3} \qquad (26)$$

Where

$$M_3 = \frac{1}{2}(V_{P3,S} + Z_{C,L3}I_{P3,S})e^{-\Gamma_{L3}L_3} - \frac{1}{2}(V_{P3,R} + Z_{C,L3}I_{P3,R}) \qquad (27)$$

$$N_3 = \frac{1}{2}(V_{P3,R} - Z_{C,L3}I_{P3,R}) - \frac{1}{2}(V_{P3,S} - Z_{C,L3}I_{P3,S})e^{\Gamma_{L3}L_3}. \qquad (28)$$

Furthermore, we can normalizeD_3 to obtain $D_{3,R}$ using the line length L_1 as reference length, such that the fault location x=$D_{3,R}L_1$ away from bus R in the form

$$D_{3,R} = \frac{\ln\left(\frac{N_3}{M_3}\right)}{2\Gamma_{L3}L_1} + \alpha_3 \qquad (29)$$

$$\alpha_3 = \frac{(L_1 + L_2)}{L_1}. \qquad (30)$$

Using the principle of mathematical induction, the general form of fault location indices D_K for all line sections can be obtained, where K=1…N are as follows:

$$D_K = \frac{\ln\left(\frac{N_K}{M_K}\right)}{2\Gamma_{LK}L_K} \qquad (31)$$

and the general normalized fault location indices $D_{K,R}$ are written as the following:

$$D_{K,R} = \frac{\ln\left(\frac{N_K}{M_K}\right)}{2\Gamma_{LK}L_1} + \alpha_K \qquad (32)$$

Where

$$M_K = \frac{1}{2}(V_{PK,S} + Z_{C,LK}I_{PK,S})e^{-\Gamma_{LK}L_K} - \frac{1}{2}(V_{PK,R} + Z_{C,LK}I_{PK,R}) \qquad (33)$$

$$N_K = \frac{1}{2}(V_{PK,R} - Z_{C,LK}I_{PK,R}) - \frac{1}{2}(V_{PK,S} - Z_{C,LK}I_{PK,S})e^{\Gamma_{LK}L_K} \qquad (34)$$

$$\alpha_K = \frac{\left(\sum_{n=1}^{K-1} L_n\right)}{L_1} \qquad (35)$$

Published By:
Blue Eyes Intelligence Engineering
and Sciences Publication (BEIESP)

where the data sets ($V_{PK,R}$, $I_{PK,R}$) and ($V_{PK,S}$, $I_{PK,S}$) expressed in (33) and (34) can be derived in terms of the data sets (V_R,I_R) and (V_S,I_S) by rewriting (22) and (24) into generalforms, as shown in the following:

$$\begin{bmatrix} V_{PK,R} \\ I_{PK,R} \end{bmatrix} = \left(\prod_{m=1}^{K-1} T_{R(K-m)} \right) \cdot \begin{bmatrix} V_R \\ I_R \end{bmatrix} \qquad (36)$$

$$\begin{bmatrix} V_{PK,S} \\ I_{PK,S} \end{bmatrix} = \left(\prod_{m=K+1}^{N} T_{Sm} \right) \cdot \begin{bmatrix} V_S \\ I_S \end{bmatrix}. \qquad (37)$$

Equations (36) and (37) are named as the measured-data converting equations for the two-terminal multisection compound transmission lines.

The Proposed Fault Section/ Fault Location Identification: So far, we have derived N fault location indices, D_K and N normalized fault location indices, . Now the problem is which fault location index set (D_K,$D_{K,R}$) is the correct set for accurately locating a fault. Theoretically, only one correct index set corresponds to a single fault. We propose an efficient searching algorithm for this purpose. The flowchart of the algorithm shown in Fig. 9 illustrates the operations of fault section/location identification strategies for two-terminal multisection compound transmission lines. The details of the algorithm are explained in the following three steps:

Step 1) Asmentioned above, bus R and the line length L_1 are selected as the receiving end and reference length. Base on the assumption that a midway fault occurs At y km away from bus R in section K, so y=$D_{K,R}L_1$.

Step 2) ***Generate the N Fault Location Index Set***

The data sets ($V_{PK,R}$, $I_{PK,R}$) and ($V_{PK,S}$, $I_{PK,S}$) can be derived by (36) and (37). Equations (31) and (32) are then applied to obtain the fault location index D_K and $D_{K,R}$, where K is from 1 to N .

Step 3) ***Searching for correct fault location index set***

Similar to the results of two-section compound lines shown in Table I, we further propose three strategies for the efficient search for the correct fault location index set

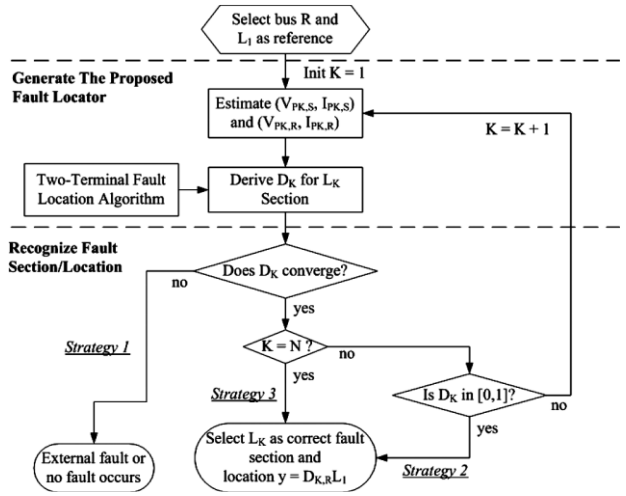

Fig. 9. The proposed fault section selector/locator for two-terminal N-section compound lines.

Strategy 1: If D_K any is an indefinite value, then an external fault or no fault occurs.

Strategy 2: From K=1 to N-1 , if the obtained D_K falls within the interval [0,1], according to the two-terminal fault location theorem [10]–[12] then D_K the is recognized as the correct fault location index and the correct fault distance y is $D_{K,R}L_1$ away from the receiving end R .

Strategy 3: Given K=N, since L_N is the last line section of the proposed fault-locating procedures, it obviously indicates the fact that D_N is identified as the correct fault location index and the correct fault distance y is $D_{N,R}L_1$ away from the receiving end R.

III. PERFORMANCE EVALUATION

A. *Simulated Cases Evaluations*

A Taipower 161 kV, transposed double-circuit four-section compound transmission line with zero sequence mutual coupling was simulated using the distributed parameter model shown in Fig. 10. The double-circuit line can be treated as two independent single-circuit lines as only positive sequence data is used in the proposed scheme. Therefore, the double-circuit line model shown in Fig. 10 was intentionally established to test the performance of the proposed fault location algorithm. LineS-T is used to evaluate the performance of the proposed scheme for external faults. The simulated system was developed using MATLAB/SIMULINK® simulator [24] with the use of Taipower 161 kV Transmission line parameters. The related parameters are summarized in Table II. All the measurements are filtered using the second-order Butterworth anti-aliasing filters with cutoff frequency of 360 Hz. The sampling frequency is 1920 Hz (32 sampling points per cycle). A digital mimic filter [27] and full-cycle DFT are employed to reduce decaying dc offset and to obtain the fundamental phasors.

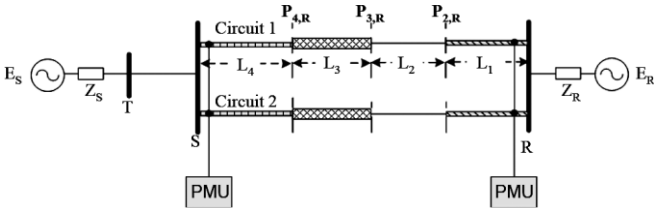

Fig. 10. The simulation system consists of a transposed double-circuit four section compound transmission line and an external line S-T.

The simulations have been conducted in reference to various system operations and fault conditions. The performance index in terms of the error percentage is defined as follows:

$$\text{Error}(\%) = \frac{|\text{estimated location} - \text{autual location}|}{\text{total line length of transmission line}} \times 100\%. \qquad (38)$$

TABLE II
PARAMETERS OF A FOUR-SECTION COMPOUND TRANSMISSION LINE SYSTEM

Published By:
Blue Eyes Intelligence Engineering and Sciences Publication (BEIESP)

System voltage : 161kV System frequency : 60Hz

Source

E_S=1.0∠10°pu E_R=1.0∠0°pu

Source impedance

Z_{S1}=0.238+j5.72 (Ω) Z_{S0}=2.738+j10(Ω)

Z_{R1}=0.238+j6.19(Ω) Z_{R0}=0.833+j5.118 (Ω)

Section length of transmission line (km):

L_1= 0.75 L_2=9.085 L_3=22.812 L_4=3.39

Bus S-Bus T=11

Transmission line parameters :

Positive-sequence:

$R_{1\ L1}$=0.016 (Ω/km) $L_{1\ L1}$=0.268 (mH/km) $C_{1\ L1}$=456.9 (nF/km)
$R_{1\ L2}$=0.038 (Ω/km) $L_{1\ L2}$=0.896 (mH/km) $C_{1\ L2}$=13.1 (nF/km)
$R_{1\ L3}$=0.048 (Ω/km) $L_{1\ L3}$=0.898 (mH/km) $C_{1\ L3}$=13.4 (nF/km)
$R_{1\ L4}$=0.061 (Ω/km) $L_{1\ L4}$=0.903 (mH/km) $C_{1\ L4}$=12.6(nF/km)
$R_{1\ BusS-T}$=0.038(Ω/km) $L_{1\ BusS-T}$=0.896(mH/km) $C_{1\ BusS-T}$=13.1(nF/km)

Zero-sequence:

$R_{0\ L1}$=0.059 (Ω/km) $L_{0\ L1}$=0.206 (mH/km) $C_{0\ L1}$=456.9 (nF/km)
$R_{0\ L2}$=0.248 (Ω/km) $L_{0\ L2}$=2.686 (mH/km) $C_{0\ L2}$=7.12 (nF/km)
$R_{0\ L3}$=0.380 (Ω/km) $L_{0\ L3}$=3.148 (mH/km) $C_{0\ L3}$=7.11 (nF/km)
$R_{0\ L4}$=0.362 (Ω/km) $L_{0\ L4}$=3.329 (mH/km) $C_{0\ L4}$=6.7 (nF/km)
$R_{0\ BusS-T}$=0.248(Ω/km) $L_{0\ BusS-T}$=2.686(mH/km) $C_{0\ BusS-T}$=7.12(nF/km)

Zero-sequence mutual coupling:

$R_{0m\ L1}$=0.004 (Ω/km) $L_{0m\ L1}$=0.015 (mH/km) $C_{0m\ L1}$=-1.427 (nF/km)
$R_{0m\ L2}$=0.209 (Ω/km) $L_{0m\ L2}$=1.535 (mH/km) $C_{0m\ L2}$=-2.896 (nF/km)
$R_{0m\ L3}$=0.330 (Ω/km) $L_{0m\ L3}$=1.994 (mH/km) $C_{0m\ L3}$=-2.866 (nF/km)
$R_{0m\ L4}$=0.282 (Ω/km) $L_{0m\ L4}$=2.153 (mH/km) $C_{0m\ L4}$=-2.038 (nF/km)

1)Selected Case: The fault-on response curves of the proposed fault location indices D_K(K=1-4) for a phase-"ab" to ground fault (ab–g fault) on the line S-T (external fault) is shown in Fig. 11(a). The fault position is set at 6.6 kmaway from bus S , the fault resistance is 1 Ohm and the fault inception angle is zero degree with respect to phase-"a" voltage waveform at bus S. Fig. 11(a) obviously shows that all of the four indices D_1-D_4 do not converge. Fig. 11(b) shows the fault-on response curves of the proposed fault location indices for a phase-"a" to ground fault (a–g fault) on the L_4 (internal fault). The fault position is set at 2.712 km (80% of the length L_4) away from , $P_{4,R}$, the fault resistance is 10 Ohm and the fault inception angle is zero degree with respect to phase-"a" voltage at bus . Fig. 11(b) demonstrates that all four indices D1-D4 converge, but only D4 falls within the interval [0,1] . According to the proposed faulted section/ fault location identification, the index D_4=0.7987 p.u. is the correct fault location, and the fault location error percentage is 0.0122%.

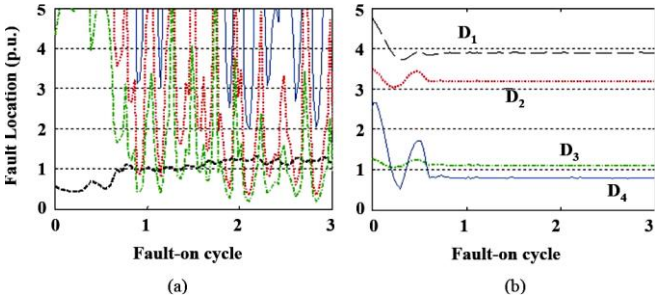

Fig. 11. The fault-on response curves of the proposed fault location indices for: (a) an external fault and (b) an internal fault on the L_4 section.

TABLE III
PERFORMANCE EVALUATION UNDER DIFFERENT FAULT POSITION SCENARIO

Line system	Fault section location	Fault type R_F	Fault location indices D_1	D_2	D_3	D_4	Fault section selector	Fault location error %
Transposed	L_1 0.15 km from bus R	AG 1Ω	**0.2042**	-1.0251	-2.4030	-9.3300	○[1]	0.0087
	L_2 3.634 km from $P_{2,R}$	BG 1kΩ [30]	3.2904	**0.4001**	-1.2375	-8.2262	○	0.0025
	L_3 17.109 km from $P_{3,R}$	ABS 50Ω	4.8237	2.8933	**0.7508**	-1.6632	○	0.0506
	L_4 3.051 km from $P_{4,R}$	ABG 10kΩ	7.2636	3.8669	1.1353	**0.9010**	○	0.0094
	External fault 1.5 km from bus S	BCG 100Ω	–[2]	–	–	–	○	–
Non-transposed	L_1 0.225 km from bus R	CG 10kΩ	**0.3107**	-2.2331	-5.3167	-8.7757	○	0.0223
	L_2 5.0 km from $P_{2,R}$	BCS 0.1Ω	3.6463	**0.5507**	-2.1779	-7.8365	○	0.0086
	L_3 15.968 km from $P_{3,R}$	ABCG 10kΩ	4.7553	2.7676	**0.7049**	-1.9960	○	0.3113
	L_4 2.712 km from $P_{4,R}$	ACG 500Ω	6.9614	3.8289	1.1203	**0.8089**	○	0.0837
	External fault 8.5 km from bus S	ACS 10Ω	–	–	–	–	○	–

[1]Symbol "○" denotes that the output of fault selection selector is correct.
[2]Symbol "–" denotes an indefinite value. R_F represents the fault resistance.

The technique developed so far is assumed for the transposed compound lines. Furthermore, the decoupled line parameters for the nontransposed transmission lines can be obtained using the manner proposed in [10], [12], and [29]. The derived line parameters are used to evaluate the performance of the proposed fault location scheme for the nontransposed lines. The selected 10 fault cases with transposed and nontransposed line systems are conducted to show the accuracy of the developed faulted line section recognition logic, where the line parameters for the nontransposed line are also obtained from the Taipower system and the related data are the same as those of transposed lines mentioned previously. The fault conditions and results are summarized in Table III. Note that in several tested cases, the fault resistance is intentionally set as high as 10 kohm . Table III indicates that the proposed technique can accurately recognize the fault section as well as locate the fault even when a high impedance fault (HIF) occurs [30]. Therefore, the proposed technique is unaffected by the fault path resistance. Moreover, we also find that only slight fault location error is introduced under a non transposed line condition.

2)Statistical Results: The same system shown in Fig. 10 is used to perform statistical evaluation. In this test, up to 406 cases including internal and external faults are conducted. Statistics under various fault conditions for transposed compound lines are shown in Table IV. One can clearly observe that the proposed faulted section/fault location scheme yields excellent performance under different fault conditions, such as different fault types, fault positions, fault resistances, prefault loads, source impedances, and fault inception angles. The average fault location error under various fault conditions is approximately 0.01407%.

Performance evaluation of the application of the proposed technique to nontransposed two-terminal multisection lines is performed in this study as well. There are up to 406 different cases including internal and external faults to be considered. The average error percentage of fault location under various fault conditions is 0.01793%. The simulation results demonstrate that the proposed technique also works effectively for the four-section nontransposed compound lines.

Published By:
Blue Eyes Intelligence Engineering
and Sciences Publication (BEIESP)

TABLE IV
STATISTICAL RESULTS OF FAULT LOCATION SCHEME FOR THE TWO-TERMINAL FOUR-SECTION TEST LINE SYSTEM

Actual fault location		Total[2] tested case	The correct number (%) of selected fault section	Average fault location error %
Fault section	Fault position (% length of the section)			
L_1	10% from bus R	29	29 (100%)	0.0142
	50% from bus R	29	29 (100%)	0.0076
	90% from bus R	29	29 (100%)	0.0106
L_2	10% from $P_{2,R}$	29	29 (100%)	0.0032
	50% from $P_{2,R}$	29	29 (100%)	0.0028
	90% from $P_{2,R}$	29	29 (100%)	0.0043
L_3	10% from $P_{3,R}$	29	29 (100%)	0.0325
	50% from $P_{3,R}$	29	29 (100%)	0.0216
	90% from $P_{3,R}$	29	29 (100%)	0.0493
L_4	10% from $P_{4,R}$	29	29 (100%)	0.0079
	50% from $P_{4,R}$	29	29 (100%)	0.0056
	90% from $P_{4,R}$	29	29 (100%)	0.0092
External fault	10% and 90% from bus S	58	58 (100%)	--[1]

[1].Symbol "--" represents an indefinite value.
[2].Total tested cases include different fault types, pre-fault loads, fault inception angles, fault resistance, and source impedances.

B.Feild Fault Events Evaluation

The proposed technique has been implemented in Taipower 345 kV and 161 kV transmission line systems. Majority of the 161 kV two-terminal transmission lines at Taipower are multisection compound transmission lines. Over 20 field test cases were evaluated during the period from February 2008 to June 2010. Except that only a few PMUs were installed in Taipower, most of Taipower transmission lines are protected by unsynchronized digital relays. All measurements from unsynchronized digital relays or PMUs with GPS failure are synchronized first by our previously proposed fault-on data synchronization algorithm [20] prior to the application of the proposed method. The average error of the total field test cases is about 1.878% compared to the average error of 10.927% provided by the digital relay fault location function. Due to space limitation, only 10 events are summarized in Table V.

TABLE V
FIELD TEST PERFORMANCE EVALUATION FOR TAIPOWER SYSTEM

Case	Voltage Level (kV)	Number of Line Sections	Fault Type	Fault Location Errors (%)	
				With the proposed technique	Relay fault location function
1	345	6	BG	0.271	6.731
2	345	2	CG	1.621	--
3	161	3	ABG	0.757	4.576
4	161	2	AG	0.029	2.898
5	161	1	CG	1.293	3.986
6	161	1	BG	1.881	9.378
7	161	4	BG	5.466	12.076
8	161	2	AG	2.454	12.251
9	161	2	BG	2.955	20.938
10	161	2	BG	1.882	4.678

Symbol "--" represents the PMUs are instead of relay recorders installed at both terminals.

From these tests, one can conclude that the proposed fault location technique potentially has better performance than existing digital relays.

IV. CONCLUSIONS

An innovative fault location technique for two-terminal multisection compound transmission lines is presented in this paper. By only the derived indices $D_1,D_2,\ldots,D_N$ for N-section (N>=2) compound lines, the faulted section/fault position can be identified correctly. Extensive simulation studies for transposed/nontransposed double-circuit lines and field fault event tests are evaluated to demonstrate that the proposed approach gives a highly accurate response under various system and fault conditions. The proposed technique has already been implemented in the Taiwan power system since the year 2008. To date, the proposed technique continues to yield excellent performance in practice.

REFERENCES

[1] D. Novosel, D. G. Hart, E. Udren, and M. M. Saha, "Fault locationusing digital relay data," *IEEE Comput. Appl. Power*, vol. 8, no. 3, pp.45–50, Jul. 1995.

[2] S. M. Brahma, "Fault location scheme for a multi-terminal transmissionline using synchronized voltage measurements," *IEEE Trans.Power Del.*, vol. 20, no. 2, pp. 1325–1331, Apr. 2005.

[3] Y. Liao andM. Kezunovic, "Optimal estimate of transmission line faultlocation considering measurement errors," *IEEE Trans. Power Del.*,vol. 22, no. 3, pp. 1335–1341, Jul. 2007.

[4] J. Izykowski,E.Rosolowski, P. Balcerek,M. Fulczyk, andM.M. Saha,"Accurate noniterative fault location algorithm utilizing two-end unsynchronizedmeasurements," *IEEE Trans. Power Del.*, vol. 25, no. 1,pp. 72–80, Jan. 2010.

[5] T. Takagi, Y. Yamakoshi, J. Baba, K. Uemura, and T. Sakaguchi, "Anew algorithm of an accurate fault location for EHV/UHV transmissionlines: Part I—Fourier transformationmethod," *IEEE Trans. PowerApp. Syst.*, vol. PAS-100, no. 3, pp. 1316–1323, Mar. 1981.

[6] T. Takagi, Y. Yamakoshi, M. Yamaura, R. Kondow, and T. Matsushima,"Development of a new type fault locator using theone-terminal voltage and current data," *IEEE Trans. Power App. Syst.*,vol. PAS-101, no. 8, pp. 2892–2898, Aug. 1982.

[7] M. Kezunovic, J. Mrkic, and B. Perunicic, "An accurate fault locationalgorithm using synchronized sampling," *Elect. Power Syst. Res. J.*,vol. 29, no. 3, pp. 161–169, May 1994.

[8] M. Kezunovic and B. Perunicic, "Automated transmission line fault analysis using synchronized sampling at two ends," *IEEE Trans. Power Syst.*, vol. 11, no. 1, pp. 441–447, Feb. 1996.

[9] C. J. Lee, J. B. Park, J. R. Shin, and Z. M. Radojević, "A new two-terminal numerical algorithm for fault location, distance protection, and arcing fault recognition," *IEEE Trans. Power Syst.*, vol. 21, no. 3, pp.1460–1462, Aug. 2006.

[10] Y. H. Lin, C. W. Liu, and C. S. Chen, "An adaptive PMU based fault detection/location technique for transmission lines with consideration of arcing fault discrimination part I : Theory and algorithms," *IEEE Trans. Power Del.*, vol. 19, no. 4, pp. 1587–1593, Oct. 2004.

[11] Y. H. Lin, C. W. Liu, and C. S. Chen, "An adaptive PMU based fault detection/location technique for transmission lines with consideration of arcing fault discrimination, part II : Performance evaluation," *IEEE Trans. Power Del.*, vol. 19, no. 4, pp. 1594–1601, Oct. 2004.

[12] C. W. Liu, K. P. Lien, C. S. Chen, and J. A. Jiang, "A universal fault location technique for N-terminal transmission lines," *IEEE Trans. Power Del.*, vol. 23, no. 3, pp. 1366–1373, Jul. 2008.

[13] C. S.Yu, C. W. Liu, S. L. Yu, and J.A. Jiang, "AnewPMUbased fault location algorithm for series compensated lines," *IEEE Trans. Power Del.*, vol. 17, no. 1, pp. 33–46, Jan. 2002.

Published By:
Blue Eyes Intelligence Engineering and Sciences Publication (BEIESP)

[14] Y. H. Lin, C. W. Liu, and C. S. Yu, "A new fault locator for three-terminal transmission lines-using two-terminal synchronized voltage and current phasors," *IEEE Trans. Power Del.*, vol. 17, no. 2, pp. 452–459, Apr. 2002.
[15] C. S. Chen, C. W. Liu, and J. A. Jiang, "A new adaptive PMU based protection scheme for transposed/untransposed parallel transmission lines," *IEEE Trans. Power Del.*, vol. 17, no. 2, pp. 395–404, Apr. 2002.
[16] J. A. Jiang, C. S. Chen, and C. W. Liu, "A new protection scheme for fault detection, direction discrimination, classification, and location in transmission lines," *IEEE Trans. Power Del.*, vol. 18, no. 1, pp. 34–42, Jan. 2003.
[17] C. S. Chen, C.W. Liu, and J. A. Jiang, "Application of combined adaptive fourier filtering technique and fault detector to fast distance protection," *IEEE Trans. Power Del.*, vol. 21, no. 2, pp. 619–626, Apr. 2006.
[18] A. A. Girgis, D. G. Hart, and W. L. Peterson, "A new fault location technique for two and three-terminal lines," *IEEE Trans. Power Del.*, vol. 7, no. 1, pp. 98–107, Jan. 1992.
[19] A. L. Dalcastagnê, S. N. Filho, H. H. Zürn, and R. Seara, "An iterative two-terminal fault-locationmethod based on unsynchronized phasors," *IEEE Trans. Power Del.*, vol. 23, no. 4, pp. 2318–2329, Oct. 2008.
[20] C. S. Yu, "An unsynchronized measurements correction method for two-terminal fault location problems," *IEEE Trans. Power Del.*, vol. 25, no. 3, pp. 1325–1333, Jul. 2010.
[21] M. Gilany, E. S. T. Eldin, M. M. A. Aziz, and D. K. Ibrahim, "An accurate scheme for fault location in combined overhead line with underground power cable," in *Proc. IEEE Power Eng. Soc. Gen. Meet.*, San Francisco, CA, Jun. 12–16, 2005, vol. 3, pp. 2521–2527.
[22] X. Yang, M. S. Choi, S. J. Lee, C. W. Ten, and S. I. Lim, "Fault location for underground power cable using distributed parameter approach," *IEEE Trans. Power Syst.*, vol. 23, no. 4, pp. 1809–1816, Nov. 2008.
[23] A.G. Phadke and J. S. Thorp, *Synchronized Phasor Measurements and Their Applications*. Berlin, Germany: Springer, 2008.
[24] Power System Blockset User's Guide The Math Works, Inc, 2002.
[25] C. A. Gross, *Power System Analysis*. New York: Wiley, 1986.
[26] "Applied protective relaying," Relay-Instrument Division, Westinghouse Electric Corp., Coral Springs, FL, 1982.
[27] G. Benmouyal, "Removal of DC-offset in current waveforms using digital mimic filtering," *IEEE Trans. Power Del.*, vol. 10, no. 2, pp. 624–630, Apr. 1995.
[28] A. L. Dalcastagnê, S. N. Filho, H. H. Zürn, and R. Seara, "An iterative two-terminal fault-locationmethod based on unsynchronized phasors," *IEEE Trans. Power Del.*, vol. 23, no. 4, pp. 2318–2329, Oct. 2008.
[29] H. W. Dommel, *EMTP Theory Book*, 2nd ed. Vancouver, BC, Canada: Microtran Power Syst. Anal. Corp, 1992.
[30] N. I. Elkalashy, M. Lehtonen, H. A. Darwish, M. A. Izzularab, and A.-M. I. Taalab, "Modeling and experimental verification of high impedance arcing fault in medium voltage networks," *IEEE Trans. Dielectrics and Electrical Insulation*, vol. 14, no. 2, pp. 375–383, Apr.2007.